PHYSICAL REVIEW B VOLUME 43, NUMBER 1 1 JANUARY 1991

Layered perovskite compounds $Sr_{n+1}V_nO_{3n+1}$ ($n=1$, 2, 3, and ∞)

Ayumi Nozaki, Hiroshi Yoshikawa, Takahiro Wada, H. Yamauchi, and Shoji Tanaka
Superconductivity Research Laboratory, International Superconductivity Technology Center, 10-13 Shinonome, 1-Chome, Koto-ku, Tokyo 135, Japan
(Received 8 August 1990)

New layered perovskite compounds $Sr_{n+1}V_nO_{3n+1}$ ($n=1$, 2, and 3) and $SrVO_3$ ($n=\infty$) were synthesized, and the physical properties of the compounds with $n=1$, 2, and ∞ were investigated. Sr_2VO_4 was semiconducting in its electrical properties and antiferromagnetic in its magnetic properties, while it was weakly ferromagnetic at low temperatures below 45 K. On the other hand, $Sr_3V_2O_7$ exhibited metallic behavior in its electrical conduction and a Pauli paramagnetism that was superimposed with a weak Curie-Weiss-type magnetism. The crystal structures and electrical and magnetic properties of $Sr_{n+1}V_nO_{3n+1}$ ($n=1$, 2, and 3) and $SrVO_3$ were compared.

I. INTRODUCTION

Since the discovery of superconductivity in the La-Ba-Cu-O system,[1] numerous experimental and theoretical studies have been reported for copper oxide superconductors. These copper oxide superconductors possess a common feature in the crystallographic structures. That is, there exists a two-dimensional array of CuO_6 (octahedron), CuO_5 (pyramid), or CuO_4 (square) clusters. For example, $(La,Ba)_2CuO_4$ has a K_2NiF_4-type structure which includes a two-dimensional array of CuO_6 octahedra.[2] It has been pointed out[3] that superconductivity in these copper oxides may be closely related to both the two-dimensional character in their crystal structures and the half-spin ($s=\frac{1}{2}$) of a Cu^{2+} ion in the two-dimensional array.

In the present study, we are concerned with a new compound series, a $Sr_{n+1}V_nO_{3n+1}$ ($n=1$, 2, and 3) and $SrVO_3$. $SrVO_3$ may be regarded as the compound with $n=\infty$ in this series. This series is expected to have similar crystallographic structures to those of $Sr_{n+1}Ti_nO_{3n+1}$.[4,5] The crystal structures of compounds of the $Sr_{n+1}V_nO_{3n+1}$ series with $n=1,2,3$ and $SrVO_3$ ($n=\infty$) are shown in Fig. 1. These structures are realized by piling up n units of the perovskitelike layer along a single axis. In the $Sr_{n+1}Ti_nO_{3n+1}$ series, the valence of Ti ions is 4+ and, therefore Ti ions have no d electrons. On the other hand, the valence of a V ion in this series is expected to be $4+$ $(=[2(3n+1)-2(n+1)]/n)$ and therefore V^{4+} ions are expected to have a half-spin. Thus, the compounds of this series possess common features, i.e., piles of the perovskitelike layer units and $s=\frac{1}{2}$ for V ions. Note that these features are also common to the known copper oxide superconductors. To date, only Sr_2VO_4 (Ref. 6) and $SrVO_3$ (Ref. 7) of the $Sr_{n+1}V_nO_{3n+1}$ series have been synthesized.

In the present work, a series of compounds, Sr_2VO_4, $Sr_3V_2O_7$, $Sr_4V_3O_{10}$, and $SrVO_3$, are synthesized, and their electrical and magnetic properties are studied.

II. EXPERIMENTAL PROCEDURE

Samples were prepared by a solid-state reaction method using $SrCO_3$ and V_2O_3 powders as starting materials. They were mixed and ground to stoichiometric compositions. The starting powders were ~99.9% pure. The mixed powder was calcined at 1400 °C in an Ar atmosphere for 2 h after being pressed into pellets. X-ray powder diffraction showed that the samples at this stage contained $Sr_3(VO_4)_2$ as an impurity phase. the calcined samples were reground and again pressed into rectangular bars of $\sim 2\times 2\times 20$ mm^3. The bars were encapsulated in evacuated silica tubes together with a reducing agent: TiO powder for Sr_2VO_4 or Ti_2O_3 for $Sr_3V_2O_7$. The encapsulated samples were fired at 1050 °C for 100 h. The final samples were obtained after several repetitions of firing with the intermediate grinding.

The crystal structures and the lattice constants were determined by an x-ray powder-diffraction method using Cu $K\alpha$ radiation. The oxygen contents of the samples were analyzed by an inert gas fusion nondispersive ir method (Horiba: EMGA-2800).[8] Electrical resistivity was measured in the temperature range 4.2–300 K using a standard dc four-probe technique and the magnetic properties were studied with a superconducting quantum interference device (SQUID) magnetometer (Quantum Design: MPM).

III. RESULTS

A. Sr_2VO_4 ($n=1$)

The powder-x-ray-diffraction pattern for Sr_2VO_4 is shown in Fig. 2(a). The diffraction peaks were successfully indexed for a tetragonal unit cell with the lattice constants $a=3.8341(1)$ Å and $c=12.57(1)$ Å. It was found that Sr_2VO_4 was of the K_2NiF_4 structure. The measured oxygen content of the sample was 3.99 ± 0.05. Therefore, the sample of Sr_2VO_4 was stoichiometric.

The temperature dependence of electrical resistivity of Sr_2VO_4 is shown in Fig. 3. It is clear that Sr_2VO_4 showed

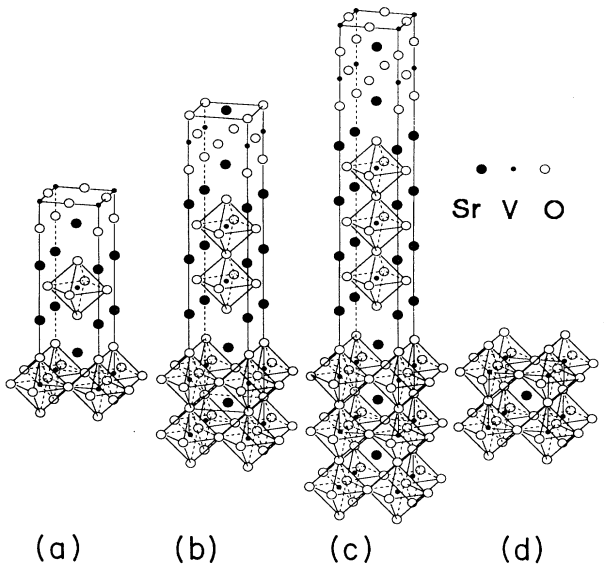

FIG. 1. Crystal structure of $Sr_{n+1}V_nO_{3n+1}$ for (a) $n=1$, (b) $n=2$, (c) $n=3$, and (d) $n=\infty$.

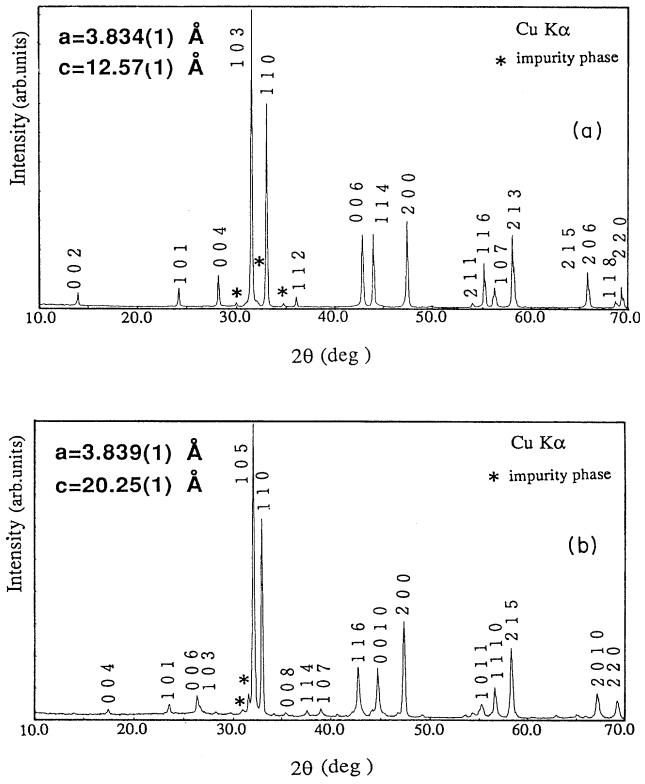

FIG. 2. Powder-x-ray-diffraction patterns for $Sr_{n+1}V_nO_{3n+1}$ with (a) $n=1$ and (b) $n=2$.

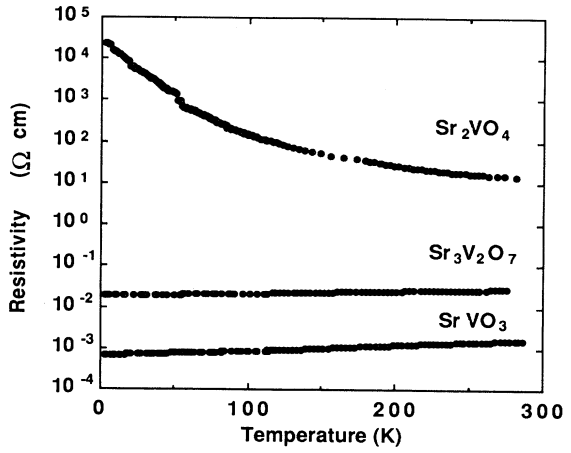

FIG. 3. Temperature dependence of electrical resistivity of $Sr_{n+1}V_nO_{3n+1}$ ($n=1$, 2, and ∞).

a semiconductive behavior and the resistivity at room temperature was about 10 Ω cm. A roughly estimated value of the activation energy for electrical conduction was between 50 and 90 meV in the temperature range 100–300 K.

The temperature dependence of magnetic susceptibility of Sr_2VO_4 is shown in Fig. 4(a). The susceptibility χ of Sr_2VO_4 was sufficiently represented by the Curie-Weiss (CW) law, i.e.,

$$\chi = C/(T-\Theta_p) ,$$

at temperatures above 100 K as demonstrated in Fig. 4(b), but it showed an unusual behavior at temperatures below 45 K, which might suggest the existence of a magnetic order at low temperatures. This magnetic order might be due to an antiferromagnetism because the resultant χ-versus-T curve angled sharply at 45 K. The Curie constant C and the Curie temperature Θ_p were determined to be 1.1×10^{-3} K emu/(g Oe) and 47 K, respectively. The effective magnetic moment per V ion calculated from the value of the Curie constant was about 1.6 times the Bohr magneton (μ_B). This value agreed with the anticipated value for an isolated V^{4+} ion ($1.73\mu_B$). The effective magnetic moment of $1.6\mu_B$ and the semiconductive electrical conduction for this material, i.e., Sr_2VO_4, indicate the existence of localized $3d^1$ electrons.

Figure 5 shows the applied magnetic-field dependence of the magnetization at 5 K. This M-versus-H curve was approximated by the superposition of a paramagnetism term and a ferromagnetism term which leveled off around 1 kOe. The value of the saturated ferromagnetic magnetization was estimated by extrapolating the M-versus-H curve to zero magnetic field. The estimated ferromagnetic moment per V ion was about $10^{-4}\mu_B$. These results suggest the existence of a weak ferromagnetism[9] in Sr_2VO_4 at low temperatures.

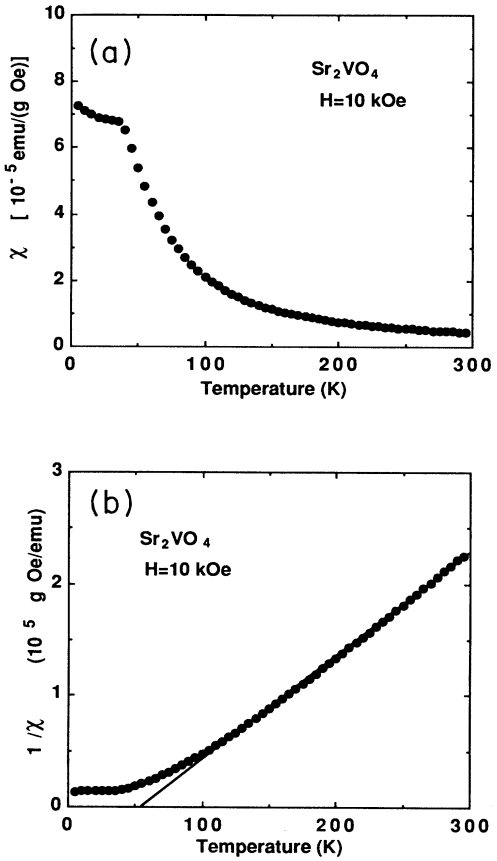

FIG. 4. Temperature dependence of magnetic susceptibility of Sr_2VO_4. Measurements were carried out on cooling at a constant field of 10 kOe. (a) Magnetic susceptibility (χ) vs temperature. (b) Reciprocal susceptibility ($1/\chi$) vs temperature. The solid line shows the extrapolation for a Curie-Weiss plot.

B. $Sr_3V_2O_7$ ($n=2$)

Figure 2(b) shows the x-ray powder-diffraction pattern for the $Sr_3V_2O_7$ sample. The diffraction peaks were indexed for a tetragonal unit cell with the lattice constants $a=3.839(1)$ Å and $c=20.25(1)$ Å. This diffraction pattern was parallel to that for $Sr_3Ti_2O_7$.[5] The oxygen content of the sample was 6.94 ± 0.05, indicating that the sample was stoichiometric $Sr_3V_2O_7$.

The temperature dependence of electrical resistivity of $Sr_3V_2O_7$ is shown in Fig. 3. The resistivity of $Sr_3V_2O_7$ was about 10^{-2} Ω cm at room temperature and slightly decreased with decreasing temperature. The compound was metallic in the electrical conduction.

Figure 6(a) shows the temperature dependence of magnetic susceptibility for $Sr_3V_2O_7$. The magnetic susceptibility of $Sr_3V_2O_7$ was approximated by a Curie-Weiss curve assuming the existence of a temperature-independent part, χ_0, in the susceptibilitiy at temperatures above 100 K. That is, χ was approximated by

$$\chi=\chi_0+C'/(T-\Theta_p') .$$

The parameters, χ_0, C', and Θ_p', estimated from Fig. 6(b),

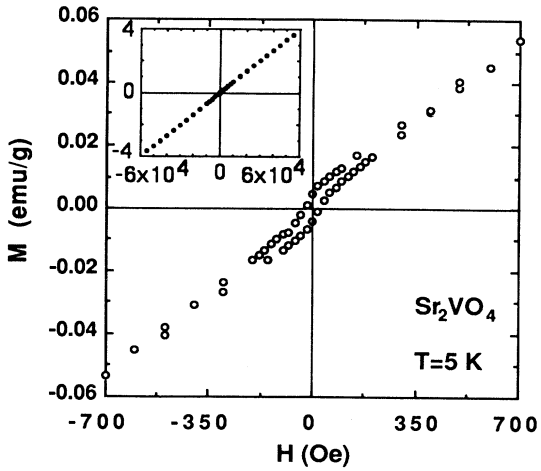

FIG. 5. Magnetization curve for Sr_2VO_4 at 5 K.

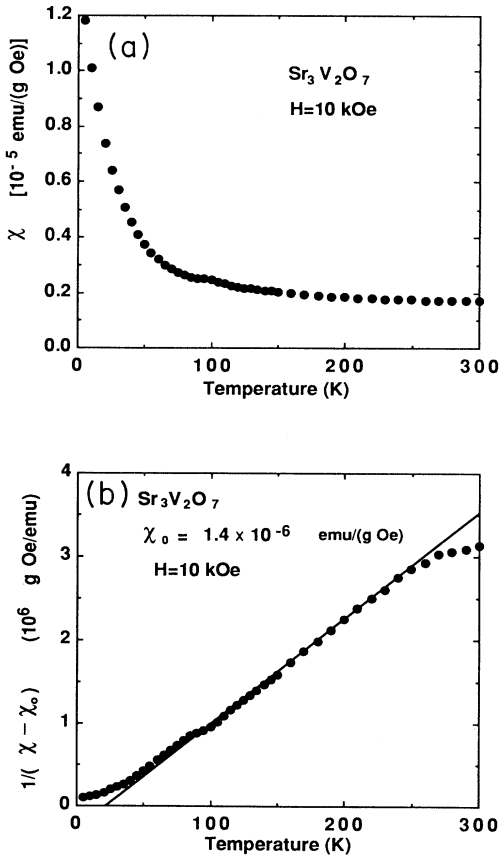

FIG. 6. Temperature dependence of magnetic susceptibility of $Sr_3V_2O_7$. Measurements were carried out on cooling at a constant field of 10 kOe. (a) Magnetic susceptibility (χ) vs temperature. (b) $1/(\chi-\chi_0)$ vs temperature with $\chi_0=1.4\times10^{-6}$ emu/g Oe. The solid line shows a fitted Curie-Weiss line.

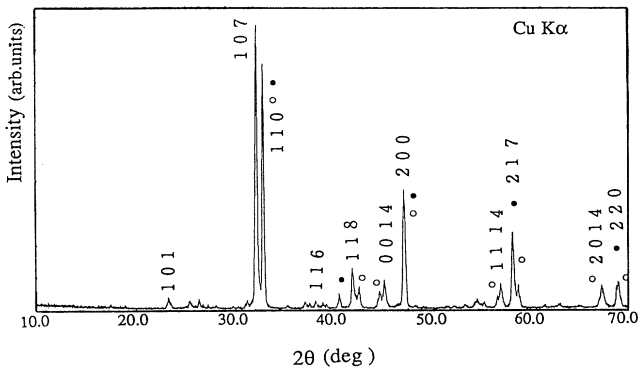

FIG. 7. Powder-x-ray-diffraction pattern for $Sr_4V_3O_{10}$ with *hkl* indices. Symbols ○ and ● are for $Sr_3V_2O_7$ and $SrVO_3$, respectively.

were 1.4×10^{-6} emu/(g Oe), 7.9×10^{-4} K emu/(g Oe), and 24 K, respectively. The effective magnetic moment per V ion was $0.4\mu_B$. It was likely that an essential feature of the magnetic property of $Sr_3V_2O_7$ was Pauli paramagnetism because $Sr_3V_2O_7$ was metallic in the electrical conduction. It was thought that the CW-type magnetism might be attributed to a narrow conduction band mainly formed by the $3d$ orbitals of V^{4+} ions, as is the case for transition metals,[10] or to stacking faults of the Sr_2VO_4-type layer (which possessed a CW-type component, as discussed in the previous section) in the crystal.

C. $Sr_4V_3O_{10}$ ($n=3$)

The x-ray powder-diffraction pattern for $Sr_4V_3O_{10}$ is shown in Fig. 7 with *hkl* indices. This sample contained $Sr_3V_2O_7$ as well as $SrVO_3$ as impurity phases. The lattice constants a and c were determined to be 3.84(1) and 27.9(1) Å, respectively.

D. $SrVO_3$ ($n=\infty$)

Single-phase samples of the perovskite type compound $SrVO_3$ were synthesized. The crystal system was cubic and the lattice constant a was 3.842(3) Å. The temperature dependence of the electrical resistivity showed a metallic behavior at temperatures between 2.5 and 300 K, and the room-temperature electrical resistivity was about 10^{-3} Ω cm as shown in Fig. 3. The data were in good agreement with those previously reported.[7]

TABLE I. Tolerance factors for the perovskite and K_2NiF_4 compounds in the Sr-V-O and Sr-Ti-O systems.

System	Perovskite ($n=\infty$)	K_2NiF_4 ($n=1$)
Sr-V-O	1.0	0.97
Sr-Ti-O	1.0	0.95

IV. DISCUSSIONS

We have demonstrated that the crystal structures of $Sr_{n+1}V_nO_{3n+1}$ compounds were parallel to those of the $Sr_{n+1}Ti_nO_{3n+1}$ compounds. The reasons why these two compound series have the same crystal structures may be discussed based on a tolerance factor (t factor) defined by

$$t=(r_A+r_0)/\sqrt{2}(r_B+r_0)\ ,$$

where r_A is the ionic radius for Sr^{2+}, r_B for V^{4+}, and r_0 for O^{2-}. For the case of the K_2NiF_4 structure (i.e., $n=1$), the Sr^{2+} radius for the coordination number $N_c=9$ was used, and for the case of the perovskite structure (i.e., $n=\infty$), the Sr^{2+} radius for $N_c=12$ was employed. The t factors calculated for the perovskite and K_2NiF_4 compounds in both Sr-V-O and Sr-Ti-O systems using the ionic radii listed in Shannon's table[11] are given in Table I. It is clearly seen inTable I that the t factors for the perovskite and K_2NiF_4 compounds of both systems are very close to unity. This means that the lattice matching between the perovskitelike layer (P layer) and the rock saltlike layer (R layer) in the K_2NiF_4 structure is nearly perfect. This feature indicates that for a $Sr_{n+1}V_nO_{3n+1}$ compound with an arbitrary integer number for n, nearly perfect lattice matching is maintained, i.e., nearly zero strain energy is involved in the formation of such a compound. This may be one of the reasons why $Sr_{n+1}V_nO_{3n+1}$ samples usually contain a multiple number of phases which would have similar levels for the free-energy.

The lattice constants of the series of $Sr_{n+1}V_nO_{3n+1}$ compounds are summarized in Table II. The length of the a axis for $Sr_{n+1}V_nO_{3n+1}$ increased with an increasing

TABLE II. Lattice constants and magnetic and electrical properties of $Sr_{n+1}V_nO_{3n+1}$ ($n=1$, 2, 3, and ∞).

Compound	n	Lattice constants a (Å)	Lattice constants c (Å)	Magnetic property	Electrical resistivity at 300K (Ω cm)
Sr_2VO_4	1	3.834(1)	12.57(1)	CW and weak ferromagnetism	10 (semiconductive)
$Sr_3V_2O_7$	2	3.839(1)	20.25(1)	Pauli-paramagnetism-like	10^{-2} (metallic)
$Sr_4V_3O_{10}$	3	3.84(1)	27.9(1)		
$SrVO_3$	∞	3.842(3)		Pauli-paramagnetism-like[a]	10^{-3} (metallic)

[a]Reference 7.

value of n. This result simply means that the lattice mismatching (between P and R layers) is the largest for the K_2NiF_4 structure ($n=1$) and nonexistent for the perovskite structure ($n=\infty$). Actually in the $Sr_{n+1}V_nO_{3n+1}$ structure, the ratio of the number of R layers to that of P layers is given by $1:n$. Therefore, as n increases, the less significant becomes the lattice mismatching. This situation obviously reflected to the values of the t factor listed in Table I.

The electrical and magnetic properties of the series of $Sr_{n+1}V_nO_{3n+1}$ compounds are also summarized in Table II. For $n=1$, i.e., Sr_2VO_4, the magnetic property was of the CW type and the electrical property was semiconductive. On the contrary, for $n \geq 2$, the compounds showed Pauli-paramagnetism-like behavior in the magnetic susceptibility and a metallic behavior in the electrical conduction. This indicates that the $3d^1$ electrons are localized in Sr_2VO_4 ($n=1$) while they are delocalized in the compounds with $n \geq 2$. In order to have $3d^1$ electrons localized in Sr_2VO_4, the magnitude of the transfer energy term W is smaller than that of the repulsion energy term U in the Hubbard Hamiltonian given by

$$H = -W + U \ .$$

When n increases from 1 to 2, since the number of V ions surrounding a V ion increases from 4 to 5, the magnitude of the W term should increase, while that of the U term is likely to remain unchanged. Thus, the state of the $3d^1$ electrons changes from a localized one to a delocalized one because the magnitude of the W term becomes larger than that of the U term when the structure changes from Sr_2VO_4 to $Sr_3V_2O_7$. In other words, the localization of $3d^1$ electrons in Sr_2VO_4 is likely to be caused by the low (or quasi-two-) dimensionality of the V-ion arrangement in the crystal stucture. The investigation on the carrier doping effects in Sr_2VO_4 is in progress.

V. CONCLUSION

Perovskite related compounds, $Sr_{n+1}V_nO_{3n+1}$ ($n=1$, 2, 3, and ∞) were successfully synthesized and their electrical and magnetic properties were characterized. Sr_2VO_4 ($n=1$) showed a Curie-Weiss behavior in the magnetic susceptibility and a semiconductive beyhavior in the electrical conduction. The coexistence of antiferromagnetism with weak ferromagnetism was suspected for Sr_2VO_4 at low temperatures. $Sr_3V_2O_7$ ($n=2$) exhibited a Paul-paramagnetism-like behavior and was metallic in the electrical property.

The properties of those series of compounds were compared and discussed in terms of the crystallographic structure. The difference in the properties of Sr_2VO_4 and $Sr_3V_2O_7$ was attributed to that in the dimensionality of the V-ion arrangements.

ACKNOWLEDGMENTS

We are grateful to Dr. K. Nakao for his helpful discussions. This work was supported by New Energy and Industrial Technology Development Organization as a part of the program for R&D of Basic Technology for Future Industries.

[1]J. G. Bednorz and K. A. Müller, Z. Phys. B **64**, 189 (1986).
[2]H. Takagi, S. Uchida, K. Kitazawa, and S. Tanaka, Jpn. J. Appl. Phys. **26**, L123 (1987).
[3]P. W. Anderson, Science **235**, 1196 (1986).
[4]S. N. Ruddlesden and P. Popper, Acta Crystallogr. **10**, 538 (1957).
[5]S. N. Ruddlesden and P. Popper, Acta Crystallogr. **11**, 54 (1958).
[6]A. Feltz and S. Schmalfuss, Z. Chem. **15**, 289 (1975).
[7]B. L. Chamberland and P. S. Danielson, J. Solid State Chem. **3**, 243 (1971).
[8]T. Wada, N. Suzuki, A. Maeda, T. Yabe, K. Uchinokura, S. Uchida, and S. Tanaka, Phys. Rev. B **39**, 9126 (1989).
[9]F. Gautier, G. Krill, M. F. Lapierre, and C. Robert, J. Phys. C **6**, L320 (1973).
[10]*Electron Correlation and Magnetism in Narrow-Band Systems,* Vol. 29 of *Springer Series in Solid State Science,* edited by T. Moriya (Springer-Verlag, Berlin, 1981).
[11]R. D. Shannon, Acta Crystallogr **A32**, 751 (1976).